diversity

MDPI

*Article*

# Endoparasitic Gall Mites: Two New *Novophytoptus* Species (Eriophyoidea, Phytoptidae) from Southern African Sedges (Cyperaceae, *Carex*) and New Hypotheses on the Phylogeny of Novophytoptines †

**Philipp E. Chetverikov [1,*], Charnie Craemer [2], Vladimir D. Gankevich [1], Maria V. Kremenetskaya [1], Igor V. Kuzmin [3] and Anna S. Zhuk [1]**

[1] Faculty of Biology, St. Petersburg State University, Universitetskaya Nab. 7/9, 199034 St. Petersburg, Russia; vd.gankevich@gmail.com (V.D.G.); mkremenetskaia@gmail.com (M.V.K.); ania.zhuk@gmail.com (A.S.Z.)
[2] Landcare Research, 231 Morrin Road, Auckland 1072, New Zealand; charniecc@gmail.com
[3] X-BIO Institute, Tyumen State University, Volodarskogo Str. 6, 625003 Tyumen, Russia; ivkuzmintgu@yandex.ru
* Correspondence: philipp-chetverikov@yandex.ru
† urn:lsid:zoobank.org:pub:E373CF37-CFD2-4A00-B25F-5004177BF77B; urn:lsid:zoobank.org:act:4E4C99C6-946D-4A33-B51F-0EC0FC4BBA68; urn:lsid:zoobank.org:act:6AFAC180-4481-4B70-90C4-9001E6CD8769.

**Abstract:** Eriophyoid mites (Acariformes, Eriophyoidea) are microscopic chelicerates morphologically greatly preadapted to endoparasitism on plants. Members of at least six phylogenetically distant eriophyoid genera from two families homoplastically transitioned to endoparasitism and acquired the ability to penetrate under the plant epidermis and feed on parenchymatous cells, usually causing necrosis. Theoretically, endoparasites are expected to show patterns of codivergence with hosts more than ectoparasites. *Novophytoptus* Roivainen 1947 is the only eriophyoid genus comprising exclusively endoparasitic species living in subepidermal tissues of herbaceous monocots of three families of the order Poales: Cyperaceae, Juncaceae, and Poaceae. Here, we described two new endoparasitic species, *N. limpopoensis* **n. sp.** and *N. zuluensis* **n. sp.,** from southern African sedges *Carex spicatopaniculata* Boeckeler ex C.B.Clarke and *C. zuluensis* C.B.Clarke, respectively, and investigated the *Cox1* phylogeny of *Novophytoptus*. Contrary to expectations, molecular phylogenetics did not recover host-specific mite clades associated with Cyperaceae and Juncaceae, but revealed geographical groups of *Novophytoptus* species from Africa and Eurasia. Our results provide a substantial basis for future coevolutionary studies on novophytoptines, which will be possible when more species and sequences of *Novophytoptus* from geographically remote regions and from diverse hosts representing all major clades of Poales become available for analyses.

**Keywords:** endoparasite; monocot; sedge; grass; rush; air-cavity; codivergence



**Citation:** Chetverikov, P.E.; Craemer, C.; Gankevich, V.D.; Kremenetskaya, M.V.; Kuzmin, I.V.; Zhuk, A.S. Endoparasitic Gall Mites: Two New *Novophytoptus* Species (Eriophyoidea, Phytoptidae) from Southern African Sedges (Cyperaceae, *Carex*) and New Hypotheses on the Phylogeny of Novophytoptines. *Diversity* **2023**, *15*, 416. https://doi.org/10.3390/d15030416

Academic Editor: Luc Legal

Received: 22 December 2022
Revised: 9 March 2023
Accepted: 10 March 2023
Published: 12 March 2023



## 1. Introduction

Mites of the superfamily Eriophyoidea Nalepa 1898 are microscopic and highly host-specific parasites permanently associated with three groups of higher vascular plants—ferns, gymnosperms, and angiosperms [1]. Up to now, this taxon includes about 5000 described species; however, recent estimates suggest that many species are still not discovered and the world fauna of Eriophyoidea may comprise up to 240,000 species [2,3]. Most known species of eriophyoids are typical ectoparasites, living as vagrants on vegetative and generative plant organs, piercing the epidermal cells by needle-shaped stylets and sucking the cell sap through their beak-like proboscis [4,5]. About 20% of species are capable of manipulating the normal development of plant organs caused by unknown factors within the saliva injected in plant cells, thereby inducing the growth of galls, and feeding on the cells of gall tissues [5–7].

Parasitism is a form of symbiotic relationship between organisms in which one (parasite) benefits at the expense of the other (host) [8]. Ectoparasites and endoparasites (including intercellular and intracellular forms) are two main groups of parasitic organisms. Intracellular endoparasites live within cells, whereas intercellular endoparasites live in the spaces between cells of the internal organs and tissues of their host. Mites (Acari) are an ancient and extremely diverse group of arachnids that have commonly exploited the parasitic niche as ectoparasites and, to a lesser extent, endoparasites of invertebrates and vertebrates [9]. Mite endoparasitism on plants is rarely discussed in the literature, and there is a tradition to classify such a relationship predominantely as a form of herbivory or "phytophagy" [10], although ecologically, it shares characteristics with endoparasitism on animal hosts.

Eriophyoids are significantly simplified and miniaturized organisms posessing only two pairs of legs, an elongated body covered with cuticular rings, a large reproductive system, well-developed central nervous system and musculature, and lacking specialized respiratory and excretory systems [4,11]. Despite their highly adaptive morphological attributes, Eriophyoidea are a very ancient, early derivative group, as evidenced by the finding of similarly morphological forms in the related superfamily Triasacaroidea in Carnian-aged amber of the Triassic Era, ca., 230 Ma [12]. Morphologically, eriophyoids are greatly preadapted to endoparasitism, especially those that possess a vermiform body resembling shapes of nematodes. Recent cladistic studies suggest that Triasacaroidea, Eriophyoidea, and their sister group, the soil mites of the early derivative family Nematalycidae, synapomorphically share a worm-like annulated opisthosoma [13–15]. This habitus could have evolved in their common ancestor as an adaptation for inhabiting narrow tunnel-like interstitial spaces in soil, making eriophyoids highly predisposed to living within plant tissues after they switched to phytoparasitism [14,16].

There is a lack of data on how common endoparasitism is in Eriophyoidea. Current data suggest that members of at least six phylogenetically remote genera (*Aceria* Keifer 1944, *Eriophyes* von Siebold 1851, *Novophytoptus* Roivainen 1947, *Oziella* Amrine et al. 2003, *Schizoempodium* Oldfield 1998, and *Trisetacus* Keifer 1952) from two families (Eriophyidae Nalepa 1898 and Phytoptidae Murray 1877) homoplastically transitioned to endoparasitism [17]. They acquired the ability to enter the tissues underneath the epidermis, reproduce in subepidermal intercellular spaces, and feed on parenchymatous cells, often causing local necrosis.

*Novophytoptus* (Phytoptidae) is the only eriophyoid genus comprising exclusively endoparasitic species living on monocots. It belongs to the monotypic phytoptid subfamily Novophytoptinae Roivainen 1953 and possesses a set of morphological traits rarely observed in other groups of eriophyoids or unique for *Novophytoptus*, some of which could have evolved as adaptations to endoparasitic life style [17,18]. *Novophytoptus* species lack gnathosomal seta *d*, tibial solenidion *φ*, and femoral setae *bv* I and II, have unusually long setae *sc* ($\geq$50 μm), eye-like structures on anterorlateral areas of the prosoma, 10–20 ventral annuli between the genital coverflap and coxae II, two pores under the genital coverflap (Figure 1F) leading to uncommonly large spermathecae (Figure 1G), and a plate-like anterior genital apodeme orthogonal to the main body axis (Figure 1G,H).

All *Novophytoptus* species live in air-cavities of leaves, leaf sheaths, and stems of herbaceous monocots of the order Poales (Figure 1A,B) and damage spongy tissues between veins. As a result, characteristic "brownish stripes" corresponding to necrotized subepidermal parenchyma appear on the infested plant organs (Figure 1C–E). Novophytoptines penetrate and exit subepidermal spaces of their hosts through circular holes (Figure 1E), which they possibly "cut" or "drill" in the epidermis, or through epidermis stomata [17,20]. However, it was shown that their stylets are unsuitable for making holes large enough for a mite to squeeze through, and the sizes of mature epidermal stomata are too small for penetration by eriophyoids [17]. Therefore, the exact mechanism of epidermal perforation is still unknown. Probably, mites attack the plant epidermis in the early stage of its development when the leaf or stem is young and a small hole initially produced by the

mite's stylets in the relatively soft, developing epidermis later enlarges to become a larger aperture. Alternatively (but less likely, we believe), the mites could kill several neighboring epidermal cells and penetrate later through the large area of the destroyed epidermis.

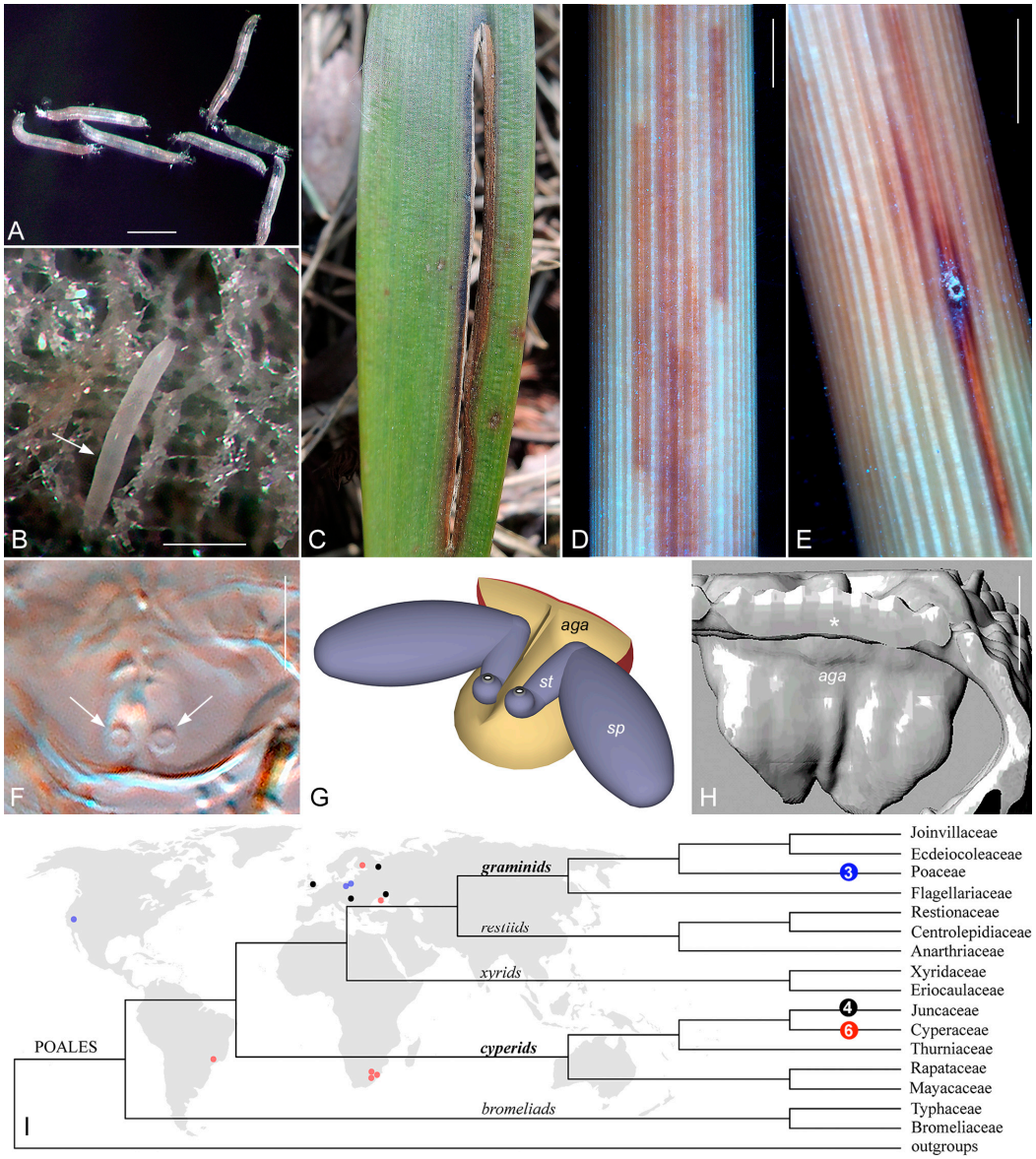


**Figure 1.** (**A**)—Group of *Novophytoptus longissimus* in a Petri dish with water, (**B**)—a female of *N. longissimus* (arrow) inside stem of *Juncus conglomeratus* (Serbia), (**C**,**D**)—necrosis of intervein leaf mesophyll caused by *N. luzulis* on *Luzula pilosa* (**C**, Northern West Russia) and by *N. rostratae* on *Scirpus* sp. (**D**, Northern West Russia), (**E**)—emergency exit in stem epidermis of *Scirpus* sp. used by *N. rostratae* for leaving subepidermal spaces, (**F**)—paired pores (arrows) leading to spermathecal tubes in *N. maritimus* (DIC LM, Ukraine), (**G**)—a generalized 3D scheme of female internal genitalia of *Novophytoptus*, (**H**)—3D reconstruction of anterior genital apodeme in *N. rostratae* (asterisk indicate ventral opisthosomal cuticle). (**I**)—Novophytoptine species diversity mapped on the phylogeny of Poales (simplified from [19]). Numbers of *Novophytoptus* species (including the two new species described in this paper) associated with Poaceae (blue), Juncaceae (black), and Cyperaceae (red) are indicated in circles. Five main lineages of Poales are indicated above branches. Type localities of *Novophytoptus* species are shown by dots (colored according to the host family) on the background world map. Scale bar: (**A**,**B**) = 200 mm; (**C**) = 5 mm; (**D**,**E**) = 2 mm; (**G**,**H**) = 5 µm. Notations: *sp*—spermatheca, *st*—spermathecal tube, *aga*—anterior genital apodeme.

Up to now, *Novophytoptus* has been recorded from two large lineages of Poales—*cyperids* and *graminids*, with most species (77%) associated with cyperid families Juncaceae and Cyperaceae and only three species (23%) with graminid family Poaceae (Figure 1I). In 2013–2017, several expeditions focused on exploring the eriophyoid fauna of South Africa were organized by the ARC Plant Protection Research Institute (Roodeplaat, Gauteng, South Africa) in cooperation with Saint-Petersburg State University (Russia). During these expeditions, special efforts were made to elucidate if *Novophytoptus* occurs in the African continent because, at that time, this genus was known only from Europe, and North and South America. Mites of this genus were not found on *Xyris* sp. (*xyrids*, Xyridaceae) sampled in 2013 in the Magaliesberg mountains near Pretoria (South Africa), nor on *Prionium serratum* (L.f.) Drège (*cyperids*, Thurniaceae) and *Restio* spp. (*restiids*, Restionaceae) sampled in 2016 near Cape Town. However, they were frequently recorded on various sedges and rushes (Cyperaceae and Juncaceae, *cyperids*) in Gauteng, Mpumalanga, Limpopo, and Western Cape provinces of South Africa in 2013, 2016, and 2017.

In this paper, we describe two new *Novophytoptus* species from African sedges, provide their *Cox1* sequences, and reconstruct a molecular phylogeny of *Novophytoptus* in order to test two hypotheses: (1) species of *Novophytoptus* cluster according to the families of their hosts, and (2) the phylogenetic relationships of *Novophytoptus* species are related to geographic proximity, more specifically to the continent on which they occur. We also examined specimens of three additional *Novophytoptus* species (including paratypes for some of them) that morphologically resemble the two new species from South Africa in order to find characterstics for separating them the most effectively.

## 2. Material and Methods

**Morphology.** Live mites used in the descriptions and phylogenetic analyses were collected in 2017 in South Africa from plants using a fine minuten pin and a dissecting microscope, and then placed in Eppendorf tubes filled with 96% ethanol. Ethanol-preserved material was used for DNA extraction and slide mounting. The mites were mounted in Hoyer's medium with iodine [21] and cleared on a heating block at 90 °C for 3–5 h. Slide-mounted specimens were examined with differential interference contrast (DIC) light microscopy (LM) using a Leica DM2500 (Leica Microsystems GmbH, Wetzlar, Germany) equipped with a digital camera, ToupCam UCMOS09000KPB. Images and specimens were analyzed and measured using ToupTek ToupView (Hangzhou ToupTek Photonics Co., Ltd., Hangzhou, China). In the descriptions of the new species, the measurements of a holotype (female) are given followed by measurement ranges for the paratype females. In the description of males, the measurements are given as ranges. All measurements are given in micrometers (μm) and are lengths, except when mentioned otherwise. The classification and terminology of the external morphology follow [2,4]. Drawings of mites were sketched by pencil using a video projector [22], scanned, and finalized in Adobe Illustrator CC 2014 (Adobe Systems, San Jose, CA, USA) using a Wacom Intuos S CTL-4100K-N (Wacom Co., Ltd., Kazo, Saitama, Japan) graphics tablet. Host plants were identified by Dr. K.W. Sepheka (SANBI, South African National Biodiversity Institute, Pretoria) and their scientific names were verified and given according to [23].

**Comparative material.** Slide-mounted females of *Novophytoptus rostratae* Roivainen 1947 from the Acarological collection of the Zoological Institute of RAS (Russia); two paratype females of *N. ammophilae* Skoracka et Boczek 2000 loaned from the Department of Animal Taxonomy and Ecology, A. Mickiewicz University (Poznan, Poland); two paratypes of *N. silvai* Flechtmann 2004 loaned from the collection of the Department of Entomology, Phytopathology, and Agricultural Zoology of the University of San-Paolo (Brazil) were used as comparative material.

**DNA extraction and sequencing.** For DNA extraction, 1–3 mite specimens of each species were crushed with a fine pin in a 3 μL drop of distilled water on a cavity well microscope slide. The drop was pipetted into a thin-walled PCR tube with 20 μL of 5% solution of Chelex® 100 Resin (Bio-Rad Laboratories, Inc., Hercules, CA, USA) before being

heated two times (5 min at 95 °C). The solution above the settled Chelex® granules was used as the DNA template for PCR to amplify a fragment of subunit I of *Cox1*. Thermal cycling profiles and primers (for PCR and for sequencing) used were as specified by [24]. After amplification, 3.5 µL of each reaction product was mixed with 0.5 µL of SYBR Green I (Lumiprobe, Hannover, Germany) and analyzed by electrophoresis in a 1% agarose gel to assess the product size and concentration. Sequences were obtained using BigDye Terminator v.3.1 chemistry in a 3500xl Genetic Analyzer (Applied Biosystems, Foster City, CA, USA). New sequences were compared with the sequences of Eriophyoidea currently available in GenBank (22 November 2022) using *blastn* and *blastx* algorithms (http://blast.ncbi.nlm.nih.gov/Blast.cgi, accessed on 22 November 2022).

**Sequence alignment and molecular phylogenetic analyses.** Apart from the two new *Cox1* sequences obtained in this study, the genus *Novophytoptus* is represented by 20 sequences of 5 genes (*Cox1*—7, *28S*—5, *18S*—4, *hsp70-5*—3, *ef1-alpha*—1) in the Nucleotide NCBI database. All available *Cox1* sequences of *Novophytoptus* were included in the analyses. *Cox1* sequences of *Oziella atherodes* Chetverikov 2011 (closely related out-group) and *Pentasetacus araucariae* Schliesske 1980 (distant out-group) were used for rooting the trees. Sequences were aligned using the L-INS-i MAFFT algorithm [25] and the web-based program interface [26] with the default settings. The absence of stop codons in *Cox1* sequences was checked with Mega 7 [27]. The *Cox1* alignment contained 11 sequences with 1166 nucleotide positions. The *Cox1* sequences were analyzed as (a) nucleotides, (b) codons, and (c) amino acids. Maximum likelihood analyses were conducted in IQ-tree 2 [28]. For gene evolution, the following models were selected using ModelFinder [29] as implemented in IQ-tree 2 based on the Bayesian Information Criterion: TIM2 + F + I + G4 (a), GY+F+R3 (b), and mtART + R2 (c). Branch support values were generated from Ultrafast bootstrap approximation (UFBoot) with 10,000 bootstrap alignments, 1000 maximum iterations, and a minimum correlation coefficient of 0.99. Values of an SH-like approximate likelihood ratio test (SH-aLRT) with 1000 replicates were labeled on the maximum likelihood (ML) trees.

## 3. Taxonomy

**Superfamily Eriophyoidea Nalepa 1898**
**Family Phytoptidae Murray 1877**
**Subfamily Novophytoptinae Roivainen 1953**
**Genus *Novophytoptus* Roivainen 1947**
**Type species: *Novophytoptus rostratae* Roivainen 1947**
**Number of species: 13.**

**Species included**: *N. aculeatus* Pye 2012, *N. ammophilae* Skoracka et Boczek 2000, *N. glyceriae* Skoracka et Boczek 2000, *N. limpopoensis* **n. sp.**, *N. longissimus* Chetverikov, Petanović 2016, *N. luzulis* Chetverikov 2015, *N. maritimus* Chetverikov 2015, *N. rostratae* Roivainen 1947, *N. silvai* Flechtmann 2004, *N. stipae* Keifer 1962, *N. tauricus* Mitrofanov, Sharonov, Sekerskaya 1983, *N. zuluensis* **n. sp.**, and *Novophytoptus* sp. (undescribed species from South Africa).

**Hosts**: sedges (Cyperaceae), rushes (Juncaceae), and grasses (Poaceae).

**Relation to hosts**: all members of this genus are endoparasites, living under the epidermis in air-cavities or in spaces of parenchymatous tissues of leaves, leaf sheaths, and stems.

***Novophytoptus ammophilae* Skoracka et Boczek 2000** (Figure 2). Two paratype females from *Ammophila arenaria* (L.) Link. (Poaceae), from POLAND: Western Pomerania, MiKdzyzdroje, on dune, 21 July 1999, slides #P1 and #P2, coll. A. Skoracka. The mites were found vagrant on leaves and causing no visible damage [30].

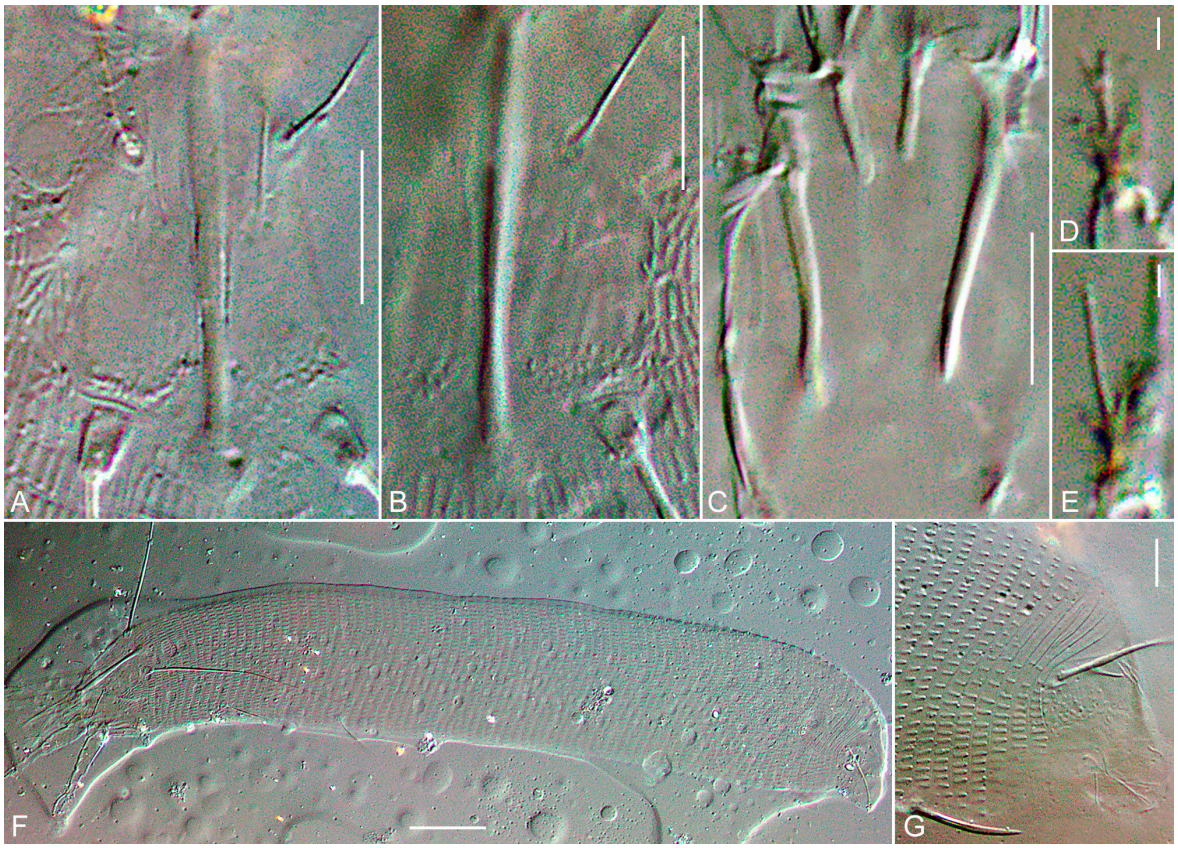


**Figure 2.** DIC LM images of two paratype females of *Novophytoptus ammophilae* Skoracka et Boczek 2000. (**A**,**B**)—prodorsal shield, (**C**)—coxal apodemes, (**D**,**E**)—empodia I (**D**) and II (**E**), (**F**)—entire female, (**G**)—dorso-lateral aspect of telosome. Scale bar: (**A**–**C**,**G**)—10 μm; (**D**,**E**)—1 μm; (**F**)—30 μm.

**Remarks.** This species has (1) the last 3–4 dorsal telosomal annuli smooth; (2) very strong coxal apodemes protruding inside body in a form of blunt rod-shaped processes; (3) indistinct lateral margins of prodorsal shield; (4) all opisthosomal setae of normal thickness except stout and thickened setae *f*; (5) two groups of microtubercles preceding tubercles of *sc* and no microtubercles in the medioposterior field of prodorsal shield; (6) almost smooth lateral areas of prodorsal shield; (7) admedian and median lines fused forming entire central ridge; (8) asymmetrical empodia: in empodium II, one of the terminal rays is about 5–6 times longer than the other; in empodium I, terminal rays are subequally long and situated on a short rod-like shaft and, thus, remote from other rays; (9) ventral surfaces of femur, genu, and tibia of both legs with thin longitudinal striae. *Novophytoptus ammophilae* is close to *N. maritimus* Chetverikov 2015. The traits (4), (6), and (7) from the list above differentiate these two species: contrary to *N. ammophillae*, in *N. maritimus*, all opisthosomal setae are notably thickened, lateral areas of the prodorsal shield with distinct sinuous lines, and median and admedian lines non-fused.

***Novophytoptus rostratae* Roivainen 1947** (Figure 3A–F). Whitish and slightly orange females and males and immatures inside air cavities under leaf epidermis of *Carex rostrata* Stokes (Cyperaceae) (type host), from FINLAND: Imatra, 61°09′52.3″ N 28°46′17.0″ E, 3 July 2012, slide series #I1/10-12, coll. P.E. Chetverikov. Damaged areas between veins of green infested leaves are brown because of necrosis of subepidermal parenchyma.

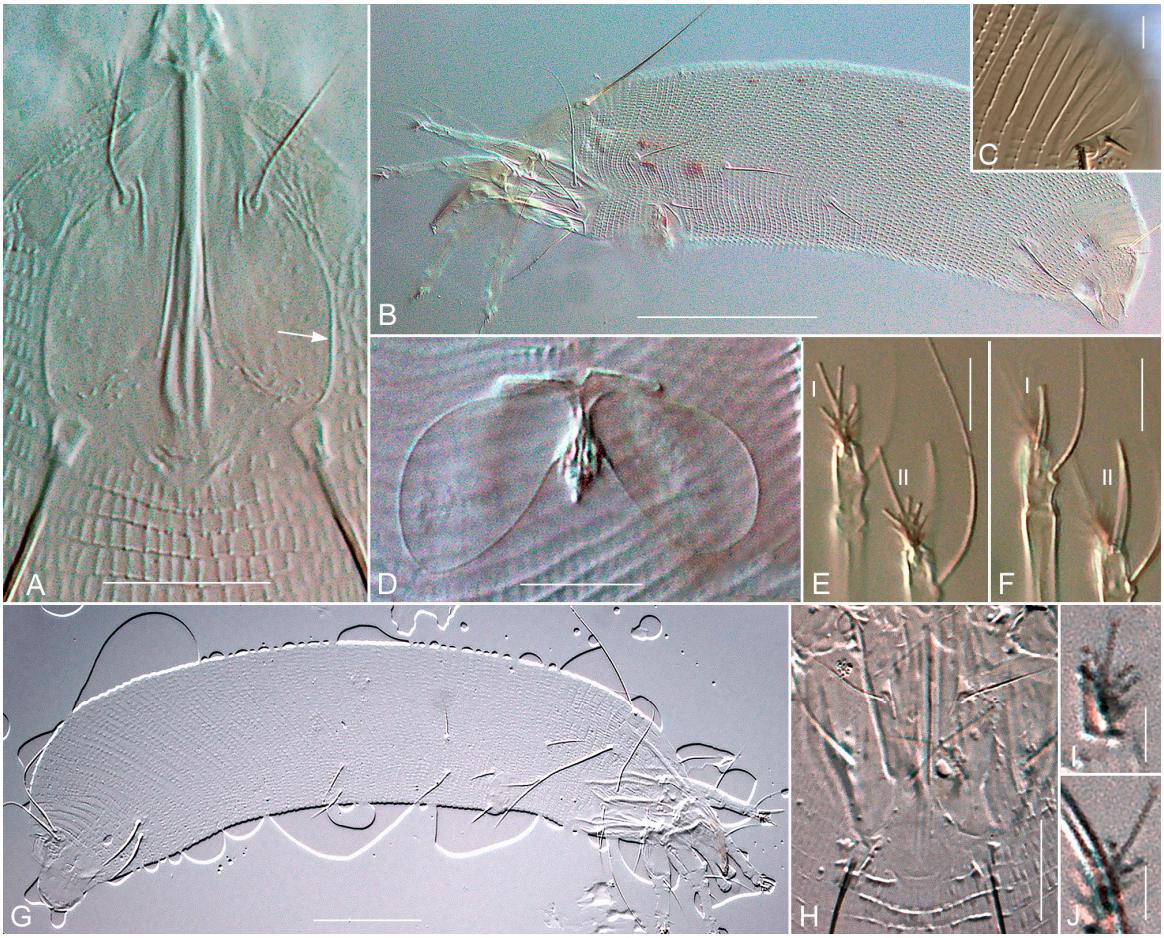


**Figure 3.** DIC LM images of females of *Novophytoptus rostratae* Roivainen 1947 (**A**–**F**) and *N. silvai* Flechtmann 2004 (**G**–**J**). (**A**)—Prodorsal shield, (**B**)—semi-lateral view of entire mite, (**C**)—smooth dorsal telosomal annuli, (**D**)—internal genitalia, (**E**)—empodia I and II, (**F**)—tarsal solenidia I and II. Scale bar: (**A**) = 15 µm; (**B**) = 50 µm; (**C**) = 3 µm; (**D**–**F**) = 5 µm; (**G**)—30 µm; (**H**)—10; (**I**,**J**)—2 µm.

**Remarks**. *N. rostratae*, the type species of the genus *Novophytoptus*, was described from a sedge *C. rostrata* from Finland in the middle of the 20th century as vagrant on leaves [31]. Later, it was shown that (a) *N. rostratae* is an endoparasite living under the leaf and stem epidermis on various hosts of cyperaceous genera *Bolbloschoenus*, *Carex*, *Eriophorum*, *Scirpoides*, and *Scirpus* in Eurasia; (b) the specimens sampled from mite populations associated with different hosts are so similar morphologically that only multivariate statistics of morphometric data can differentiate them [32,33]. Considering the unusually large and diverse list of hosts, this taxon may be a complex of cryptic species such as *Aceria tosichella* Keifer or *Abacarus hystrix* (Nalepa) from grasses [34,35]. The diagnostic traits of *N. rostratae* are: (1) distinct ridge delimiting lateral margin of prodorsal shield; (2) higher body width/length ratio because the mite is more robust, thick, and wide in comparison to some other members of *Novophytoptus*, e.g., *N. stipae*, *N. longissimus*, *N. maritimus*, and *N. luzulis*, which have more elongated, worm-like bodies; (3) smooth dorsal telosomal annuli; (4) median and admedian lines completely fused into a solid thick ridge in anterior third of prodorsal shield but distinctly diverging in posterior half of the shield; (5) differently shaped empodia I (symmetrical, the terminal fork close to the shaft) and II (asymmetrical, one of the terminal rays is about 3-4 times longer than the other); (6) femur and genu of both legs with thin longitudinal striae ventrally, while tibiae I and II smooth ventrally. The combination of characteristics (1), (2), (3), and (6) separates *N. rostratae* from all other species of *Novophytoptus*.

***Novophytoptus silvai* Flechtmann 2004** (Figure 3G–J). Two paratype females from *Cyperus giganteus* Vahl. (Cyperaceae), from BRAZIL: Sao-Paolo, Pariquera-acu, 24°36′51″ S, 47°33′22″ W, 7 October 2003, slides #17 and #19 from series #2650, coll. L.V.F. Silva. The mites were found vagrant on leaves and inflorescences and " . . . in the spaces inside older leaves, intralaminar, from where they emerge, in large numbers, through cuticular holes cut in the leaf epidermis" [20].

**Remarks**. The two investigated paratype slides are in poor condition: the medium contains cracks, grains, and bubbles; the paratype specimens are overly flattened and mite exoskeletons are so translucent that topographies of dorsal and ventral cuticles are visually merged and could hardly be discerned from each other (Figure 3G,H). However, it was possible to ascertain that (1) lateral margins of the prodorsal shield are indistinct and the ridges, which were observed in *N. rostratae*, are absent (Figure 3H vs. Figure 3A); (2) the shape of opisthosoma is similar to that in *N. rostratae*; (3) dorsal telosomal annuli are smooth; (4) median and admedian lines converge in anterior third of prodorsal shield forming entire thick ridge; (5) both empodia I and II are asymmetrical because their terminal rays are not equal in length; this difference is more pronounced in empodium II; (6) three parallel lines between tubercles of *ve* and *sc*, depicted in drawings of *N. silvai* in the original description, are absent in paratypes; however, similarly shaped ridges on coxal plates II are present and can be observed through dorsal cuticle, providing the false impression that they are lines of the prodorsal shield. Among all *Novophytoptus* spp., *N. silvai* is morphologically closest to *N. rostratae*. Traits (1) and (5) from the list above differentiate these two species most effectively.

***Novophytoptus zuluensis* n. sp. Female holotype** (***n* = 10,** Figure 4A–G, Figures 5, 6 and 7A–C). Idiosoma vermiform, 301 (284–312), 37 (36–41) wide at the level of setae *c2*, 45 (43–48) wide at the level of setae *f*. **Prodorsal shield** subpentagonal, 22 (21–24), 16 (15–17) wide with two ocella-like spots (="eye-like structures" sensu [36]) lateral to setae *ve*. Median line of prodorsal shield faint and short, present only in the median part of the shield. Admedian lines complete, slightly converging midway and forming entire thick ridge (under DIC LM). Three short, curved lines (submedian I, II, and III) between admedian and tubercle of *ve* and one oblique line (submedian IV) lateral to tubercles of *ve*. A pair of thin (sometimes poorly distinct) L-shaped lines, flanking admedian ridges in their posterior half, and posterolaterally reaching near *sc* tubercles; sparse microtubercles along the base of L-shaped lines. Two short converging ridges (somewhat forming a "v") preceding first dorsal opisthosomal annulus in the center. Setae *ve* 11 (10–16), directed anterolaterad, tubercles 9 (8–10) apart; *sc* 66 (60–79), directed posterolaterad, tubercles 14 (14–17) apart. Distance between tubercles *ve–sc* 14 (14–16). **Gnathosoma** elongate, directed straight forward at slightly ventral angle, 21 (20–22); pedipalp coxal seta *ep* 2 (2–3), pedipalp genual seta *d* absent, subapical pedipalp tarsal seta *ν* 0.5 (0.5–1). Ventrally, basal gnathosoma covered by rectangular suboral plate (*n* = 4) about 9–10, 5–6 wide, with two ridges forming V-shaped figures.

**Leg I** 25 (24–29), tarsus 4 (4–5), *u′* 3 (2–3), *ft′* 3 (3–5), *ft″* 11 (9–12), *ω* with tiny terminal spherical knob, 4 (4–5), empodium I 4/4-rayed, 5 (5–6), each ray of the three basal pairs with one additional secondary branch, terminal paired rays without additional branching, medial terminal ray 2–3 times longer than lateral (thus, empodium I is distinctly asymmetrical); tibia 6 (6–8), smooth ventrally, *l′* 4 (4–5), genu 4 (3–4), ventrally with 3-4 indistinct longitudinal striae, *l″* 11 (10–14), femur 8 (7–9), ventrally with 5-8 longitudinal striae, *bv* absent. **Leg II** 23 (22–28), tarsus 4 (4–5), *u′* 2 (2–3), *ft′* 3 (3–4), *ft″* 14 (13–17), *ω* with tiny terminal spherical knob, 8 (7–9), empodium II 4/4-rayed, 7 (6–8), each ray of the three basal pairs with one additional secondary branch, terminal paired rays without additional branching, medial terminal ray 3–4 times longer than lateral (thus, empodium II is distinctly asymmetrical); tibia 5 (5–7), smooth ventrally, genu 3 (3–4), ventrally with 3–5 indistinct longitudinal striae, *l″* 11 (10–14), femur 7 (7–8), ventrally with 5–7 longitudinal striae, *bv* absent.

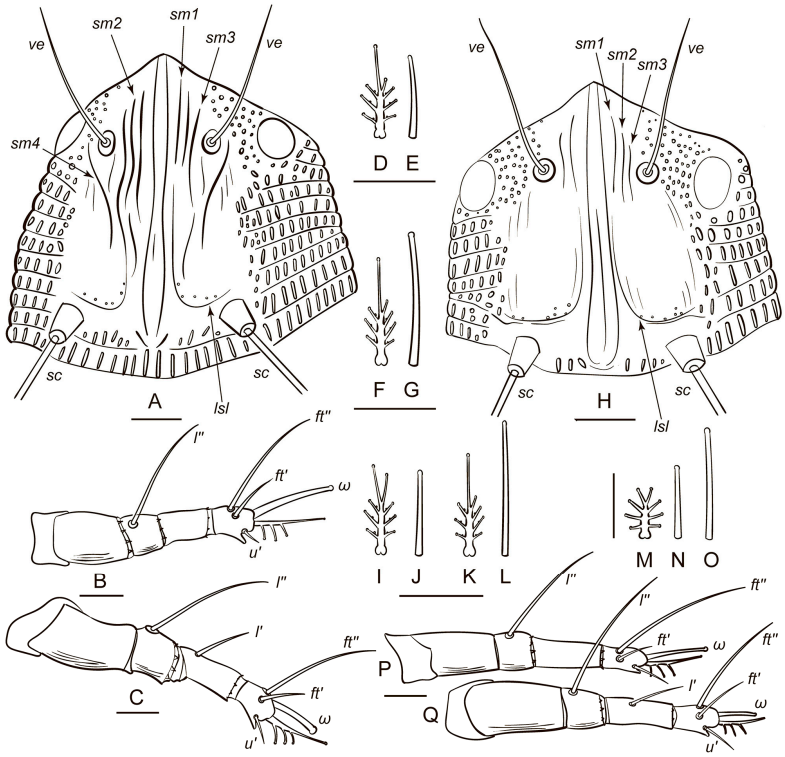


**Figure 4.** Drawings of prodorsal shields, legs, and tarsal appendages of *Novophytoptus zuluensis* **n. sp.** (**A**–**G**) and *N. limpopoensis* **n. sp.** (**H**–**Q**). (**A**)—Female prodorsal shield, (**B**,**C**)—legs II and I, (**D**)—empodium I, (**E**)—tarsal solenidion I, (**F**)—empodium II, (**G**)—tarsal solenidion II, (**H**)—female prodorsal shield, (**I**)—empodium I, (**J**)—tarsal solenidion I, (**K**)—empodium II, (**L**)—tarsal solenidion II, (**M**)—male empodium I, (**N**,**O**)—male tarsal solenidia I and II, (**P**,**Q**)—legs I and II. Scale bar 5 μm. Notations of lines of prodorsal shield (**A**): *sm1*, *sm2*, *sm3*, and *sm4*—submedian I, II, III, and IV lines; *lsl*—L-shaped line.

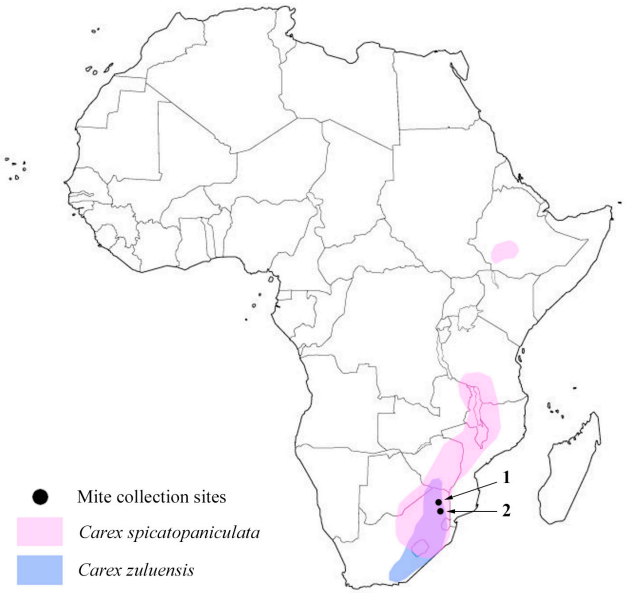


**Figure 5.** *Estimated* distributions of *Carex spicatopaniculata* and *C. zuluensis* (based on open data source from www.gbif.org, *africanplantdatabase.ch*, and www.inaturalist.org accessed on 22 November 2022) and collection sites of *N. limpopoensis* **n. sp.** (1) and *N. zuluensis* **n. sp.** (2) in Africa.

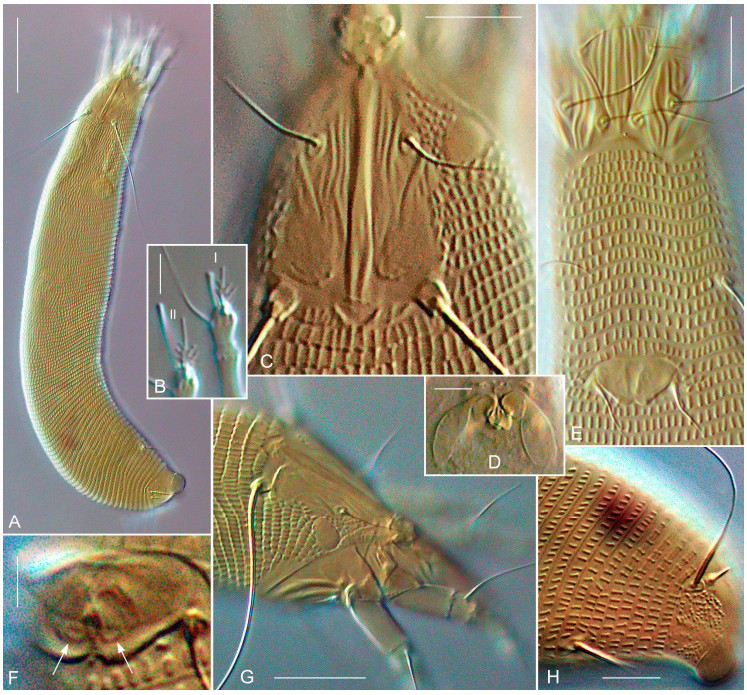


**Figure 6.** DIC LM images of *Novophytoptus zuluensis* **n. sp.** (females). (**A**)—dorsal view of entire mite, (**B**)—tarsal appendages I and II, (**C**)—prodorsal shield, (**D**)—internal genitalia, (**E**)—coxigenital area, (**F**)—two pores (arrows) leading to spermathecal tubes, (**G**)—lateral view of prosoma, (**H**)—telosome. Scale bar: (**A**) = 40 µm, (**B**) = 4 µm, (**C**,**E**,**H**) = 10 µm, (**D**) = 5 µm, (**F**) = 2 µm, (**G**) = 15 µm.

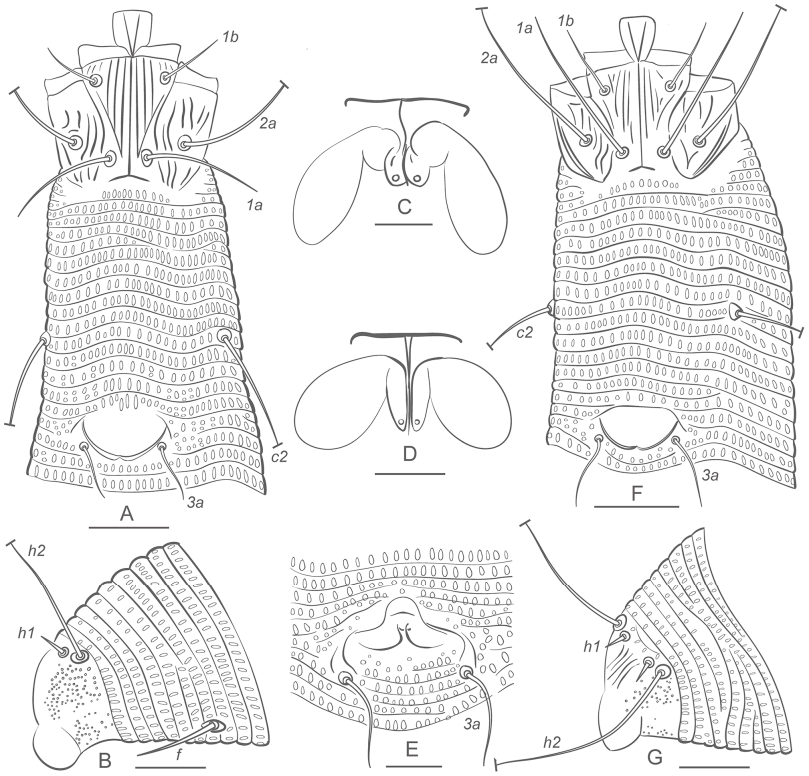


**Figure 7.** Drawings of coxigenital area (**A**,**F**), telosome (**B**,**G**), female internal genitalia (**C**,**D**), and male genital area (**E**) of *Novophytoptus zuluensis* **n. sp.** (**A**–**C**) and *N. limpopoensis* **n. sp.** (**D**–**G**). Scale bar: (**A**,**B**,**F**,**G**) = 10 µm; (**C**–**E**) = 5 µm.

Ornamentation of coxal plates variable, usually coxae I each ornamented with 3 long parallel ridges forming together a distinct pattern comprising 6 almost parallel lines, coxae II each ornamented with 5–6 sinuous longitudinal lines. Prosternal apodeme inversely T-shaped, 17 (16–18). Setae *1b* 10 (9–13), 10 (9–10) apart; *1a* 17 (16–24), 4 (4–6) apart; *2a* 32 (29–38), 16 (16–18) apart; 15 (13–16) coxigenital annuli before epigynium, pregenital plate (sensu [37]) absent. **Genital coverflap** semi-circular, smooth, 5 (5–6), 11 (10–13) wide; setae *3a* 9 (8–12), 11 (10–13) apart. Two small cuticular rings 1–1.5 in diameter, delimiting two pores leading to spermathecal tubes present under genital coverflap (Figure 5F). **Internal genitalia (*n* = 5)**. Spermatheca sac-shaped, large, 8–11, 5–7 wide; spermathecal tube curved, 4–5, consisting of two globose segments, longitudinal bridge 6–8, anterior genital apodeme, 10–12 wide, situated in transverse plane.

**Opisthosoma** vermiform, slightly expanded caudally, widest at level of tubercles *f*, with 110 (104–116) dorsal and 92 (84–100) ventral annuli with elongated microtubercles; last 5–6 dorsal annuli with less numerous and smaller microtubercles. Lateral surface of caudal lobe with group of small round microtubercles. Setal lengths: *c2* 15 (13–27), *d* 20 (18–24), *e* 10 (9–11), *f* 11 (9–13), *h1* 3 (3–4), *h2* 52 (50–66); 12 (10–13) annuli from rear shield margin to *c2*; 14 (13–15) annuli between *c2*–*d*; 22 (20–25) annuli between *d* and *e*; 38 (36–41) annuli between *e* and *f*; 6 (5–6) annuli between *f* and *h1*.

**Male**. Not found.

**GenBank data.** *OP730708 (Cox1, 1166 bp)*.

**Host plant**. *Carex zuluensis* C.B.Clarke (Cyperaceae).

**Remarks**. The host plant, *C. zuluensis*, is a robust perennial caespitose herb, 60 (80)–100 (120) cm tall with short woody rhizome, smooth, leafy stems, dark green leaves, 0.6–1.2 cm wide, glabrous, coriaceous, with scabrid margins and paniculate, lax, oblong inflorescence, 20–40 cm long. This sedge is common in South Africa, Lesotho, and the Kingdom of Eswatini (previously Swaziland), and also found in Kenya, Tanzania, and Zimbabwe (Figure 5). Typical habitats are forest margins, swampy places, e.g., stream banks. It is also often found in open grassland, on steep east- and south-facing grassy mountain slopes at 500–2100 m alt. Flowering period June–July [23,38].

**Relation to the host**. Mites live under the leaf epidermis within spaces (air-cavities) of parenchyma, where they feed on parenchymatous cells. Such feeding causes necrosis of tissues, resulting in a brownish color of the parenchyma and the inner surface of epidermis of the infested leaf area.

**Type locality**. SOUTH AFRICA: Whiskey Creek, road Sabie-Lydenburg, 16 November 2017, 25°07′40.1″ S 30°35′46.8″ E.

**Type material**. Female holotype on slide E4703, 10 paratype females on slides E4709–E4712 recovered from vial M147a containing about 40 mites in 96% ethanol. All specimens from SOUTH AFRICA (type locality), 16 November 2017, coll. P. Chetverikov, S. Neser, C. Craemer.

**Etymology**. The specific epithet, *zuluensis*, is an adjective of masculine gender, corresponding to the name of the type host plant (*C. zuluensis*) of the new species.

**Differential diagnosis.** The new species is close to *N. stipae* Keifer 1962. The main differences are in microtuberculation of the dorsal telosomal annuli (absent in *N. stipae*), lengths of setae *sc* (60–79 vs. 78–138), *ft″* II (19–25 vs. 13–17), *e* (14–21 vs. 9–11), and *f* (17–21 vs. 9–13); all setae are longer in *N. stipae* and in the ornamentation of the prodorsal shield (Figures 4A and 6C). In *N. zuluensis* **n. sp.,** the prodorsal shield has: almost smooth lateral areas (distinctly wrinkled in *N. stipae*), oblique and L-shaped lines (absent in *N. stipae*), median line very short (longer and present in posterior half of prodorsal shield in *N. stipae*), no microtubercles in the medioposterior area of prodorsal shield delimited anteriorly by L-shaped lines (medio-posterior third of prodorsal shield densely microtuberculate in *N. stipae*).

***Novophytoptus limpopoensis* n. sp. Female holotype** (***n* = 9**, Figure 4H–Q, Figure 7D–G and Figure 8). Idiosoma vermiform, 261 (256–272), 41 (40–44) wide at the level of setae *c2*, 44 (42–48) wide at the level of setae *f*. **Prodorsal shield** subpentagonal, 24 (22–26), 16 (15–18) wide with two ocella-like spots (="eye-like structures" sensu [36]) lateral to setae *ve*. Median line of prodorsal shield distinct, present in posterior half of the shield. Admedian lines complete,

slightly converging in anterior third and forming entire thick ridge (under DIC LM). Two–three short, curved lines (submedians I, II, and III) between admedian and tubercle of *ve*. Two thin mirrored L-shaped lines and sparse microtubercles along them delimiting anterolaterally a subtriangular area situated between tubercles of *sc* and posterior margin of prodorsal shield. Thin arc-shaped line between posterior margin of prodorsal shield and posterior ends of admedian and median lines. Thin short striae near lateral margin of prodorsal shield. Setae *ve* 14 (12–18), directed anterolaterad, tubercles 8 (7–9) apart; *sc* 72 (65–83) long, directed posterolaterad, tubercles 13 (12–16) apart. Distance between tubercles *ve*–*sc* 15 (14–16). **Gnathosoma** elongate, directed straight forward at slightly ventral angle, 21 (20–23); pedipalp coxal seta *ep* 3 (3–4), pedipalp genual seta *d* absent, subapical pedipalp tarsal seta *v* 0.5 (0.5–1). Ventrally, basal gnathosoma covered by elongated rectangular suboral plate with two ridges forming V-shaped figure.

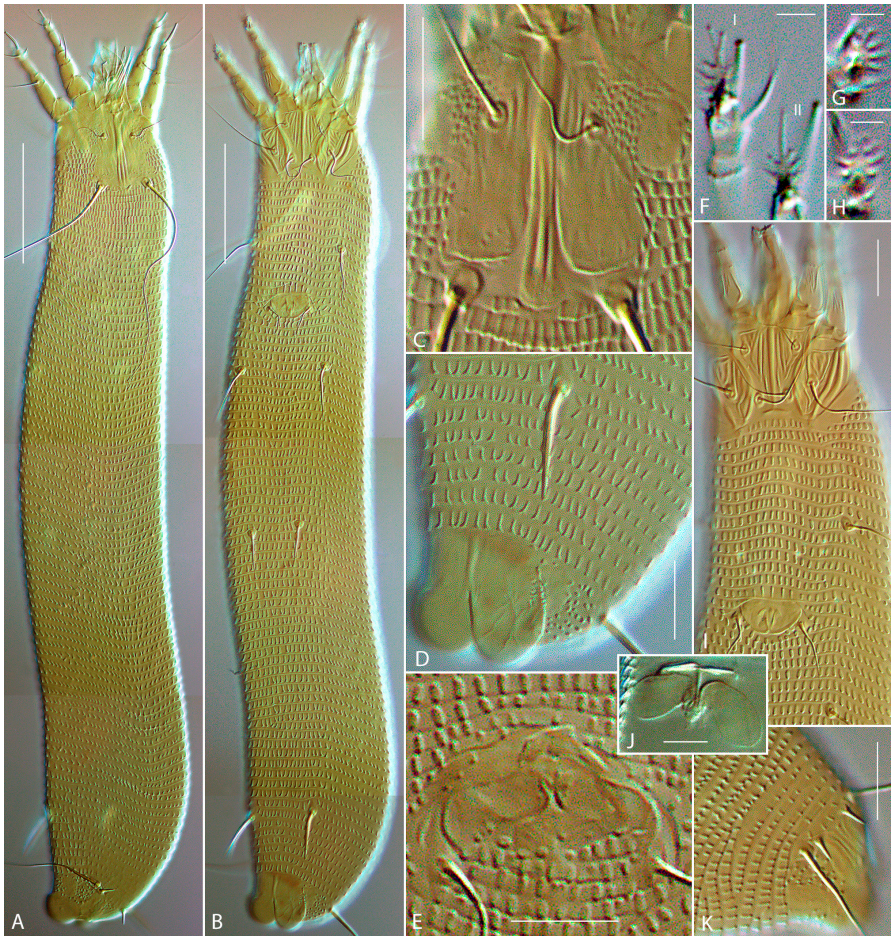


**Figure 8.** DIC LM images of *Novophytoptus limpopoensis* **n. sp.** (**A**,**B**)—dorsal (**A**) and ventral (**B**) view of entire mite, (**C**)—prodorsal shield, (**D**)—ventral aspect of anal lobe, (**E**)—male genital area, (**F**)—female tarsal appendages I and II, (**G**,**H**)—male empodia I (**G**) and II (**H**), (**I**)—female coxigenital area, (**J**)—female internal genitalia, (**K**)—semilateral view of telosome. Scale bar: (**A**,**B**) = 40 µm; (**C**,**D**), (**I**,**K**) = 10 µm; (**E**,**J**) = 5 µm; (**F**,**G**,**H**) = 2 µm.

**Leg I** 27 (25–30), tarsus 4 (4–5), $u'$ 3 (3–4), $ft'$ 4 (4–6), $ft''$ 10 (9–13), $\omega$ with tiny terminal spherical knob, 4 (4–5), empodium I 4/4-rayed, 6 (5–6), each ray of the three basal pairs with one additional secondary branch, terminal paired rays without additional branching, of equal length or medial ray slightly longer than lateral ray (thus, empodium I is almost symmetrical); tibia 7 (6–8), smooth ventrally, $l'$ 5 (4–7), genu 5 (4–5), with 3–4 longitudinal striae ventrally, $l''$ 15 (12–17), femur 8 (7–9), with 5–7 longitudinal striae ventrally, *bv* absent. **Leg II** 26 (23–27), tarsus 4 (4–5), $u'$ 3 (3–4), $ft'$ 3 (3–4), $ft''$ 15 (14–17), $\omega$ with tiny

terminal spherical knob, 7 (6–8), empodium II 4/4-rayed, 7 (6–7), each ray of the three basal pairs with one additional secondary branch, terminal paired rays without additional branching, medial terminal ray 3–4 times longer than lateral (thus, empodium II is distinctly asymmetrical); tibia 6 (5–6), smooth ventrally, genu 4 (3–4), with 3–4 longitudinal striae ventrally, *l″* 11 (10–14), femur 9 (7–9), with 4–8 longitudinal striae ventrally, *bv* absent.

Ornamentation of coxal plates variable; in most specimens, coxae I each with 2–3 longitudinal lines and 2–4 faint shorter lines, coxae II each with two distinct lateral lines and shorter irregularly oriented internal lines. Prosternal apodeme inversely T-shaped, 16 (15–17). Setae *1b* 10 (9–12), 10 (9–11) apart; *1a* 21 (20–26), 5 (5–7) apart; *2a* 40 (36–47), 17 (16–18) apart; 14 (13–15) coxigenital annuli before epigynium, pregenital plate (sensu [37]) absent. **Genital coverflap** semi-circular, smooth, 6 (5–7), 12 (10–13) wide; setae *3a* 12 (10–13), 12 (11–13) apart. Two small pores 1.5–2 in diameter leading to spermathecal tubes present under genital coverflap (not shown). **Internal genitalia (*n* = 4)**. Spermatheca sac-shaped, large, 9–12, 5–7 wide; spermathecal tube sausage-like, 3–4, longitudinal bridge 5–8, anterior genital apodeme, 11–12 wide, situated in transverse plane.

**Opisthosoma** vermiform, slightly expanded caudally, widest at level of tubercles *f*, with 88 (83–90) dorsal and 76 (72–85) ventral annuli with elongated microtubercles; last 4–5 dorsal annuli with less numerous and smaller microtubercles. Lateral surface of caudal lobe with group of small round microtubercles, 4–5 short thin longitudinal ridges between *h1*. Setal lengths: *c2* 21 (19–24), *d* 11 (9–12), *e* 12 (10–13), *f* 15 (13–17), *h1* 3 (2–4), *h2* 56 (51–71); 9 (9–10) annuli from rear shield margin to *c2*; 14 (13–16) annuli between *c2* and *d*; 18 (17–21) annuli between *d* and *e*; 29 (26–32) annuli between *e* and *f*; 6 (6–7) annuli between *f* and *h1*.

**Male (*n* = 3)**. Body elongate, 209–220, 38-42 wide, leg I 23–25, leg II 21–22, empodia I and II uniform, symmetrical, 4/4–rayed, 3–4, notably smaller than in females mainly because of the shorter terminal rays. Genital area 7–8, 10–12 wide, setae *3a* 9–11, 12–14 apart, setae *eu* not visible. Opisthosoma with 78–84 dorsal and 76–79 ventral annuli.

**GenBank data.** OP730707 (Cox1, 1152 bp).

**Host plant**. *Carex spicatopaniculata* Boeckeler ex C.B.Clarke (Cyperaceae).

**Remarks**. The host plant, *C. spicatopaniculata,* is a slender perennial caespitose herb 30–120 (140) cm tall with short thick rhizome, glabrous, leafy stems, dark green leaves, 20–50 cm long and 0.5–1.3 cm wide, with scabrid margins and veins, and paniculate inflorescence, with densely pubescent axes and branches. This sedge is common in South Africa, Lesotho, Kingdom of Eswatini, also found in Zimbabwe, Malawi, Tanzania, Ethiopia, Cameroon, and Comoros (Figure 5). It grows at an altitude of 900–3000 m. Typical habitats are forest margins. Flowering period June–July [38–40]. Botanists report that in herbaria, *C. spicatopaniculata* (the host of *N. limpopoensis* **n. sp.**) is often confused with *C. zuluensis* (the host of *N. zuluensis* **n. sp.**), *C. chlorosaccus*, *Schoenoxiphium rufum* Nees, and *S. ludwigii* [23,38]. Unverified old data suggest possible hybridization between *C. spicatopaniculata* and *C. zuluensis* [41] although later authors question this [23].

**Relation to the host**. Mites live under the leaf epidermis within spaces (air-cavities) of parenchyma, where they feed on parenchymatous cells and cause necrosis of tissues, resulting in a brownish color of the parenchyma and the inner surface of the epidermis of the infested leaf area.

**Type locality**. SOUTH AFRICA: Limpopo, Lekgalameetse National Reserve, near pools, 10 November 2017, 24°12′00.4″ S, 30°20′19.2″ E.

**Type material**. Female holotype on slide E4713, 9 paratype females and 6 males in slides E4714–E4718 recovered from vial M65a containing about 50 mites in 96% ethanol. All specimens from SOUTH AFRICA (type locality), 10 November 2017, coll. P. Chetverikov, S. Neser, C. Craemer.

**Etymology**. The specific epithet, *limpopoensis*, is an adjective of masculine gender, corresponding to the Limpopo province of South Africa, where the type locality of the new species is situated.

**Differential diagnosis.** Novophytoptus limpopoensis **n. sp.** is close to *N. zuluensis* **n. sp.** (see above). The main differences are in the ornamentation of the prodorsal shield and

coxae, number of opisthosomal annuli, and length of opisthosomal seta *d*. *Novophytoptus limpopoensis* **n. sp.** has longer median line that extends along the posterior half of the prodorsal shield, lacks the oblique line lateral to tubercles of *ve*, has thin arc-shaped line near posterior margin of prodorsal shield, two thick lateral ridges on coxae II, fewer dorsal (83–90) and ventral (72–85) annuli, and shorter opisthosomal seta *d* (9–12). *Novophytoptus zuluensis* **n. sp.** has very short median line, distinct oblique line lateral to tubercles of *ve*, two short converging ridges near posterior margin of prodorsal shield, no paired thick lateral ridges on coxae II, greater number of dorsal (104–116) and ventral (84–100) annuli, and longer seta *d* (18–24). *Novophytoptus limpopoensis* **n. sp.** is also close to *N. rostratae*, but can be easily distinguished from that by microtuberculate dorsal opisthosomal annuli (smooth in *N. rostratae*), indistinct lateral margin of prodorsal shield (delimited by distinct ridge in *N. rostratae*), and notably more elongate body (Figure 3B vs. Figure 8A,B).

**Blast search results and *Cox1* sequence diversity.** Blast searches for sequences OP730707 and OP730708 of the two new species return as the best hits the same three sequences KY922365 (*N. rostratae*), MT712729 (*N. longissimus*), and MT712730 (*N. luzulis*) with 82.32–83.45% identity when using the *blastn* algorithm and sequences ATY50385 (*N. rostratae*), QLD94603 (*N. longissimus*), and QLD94603 (*N. luzulis*) with 91.08–95.60% identity when using the *blastx* algorithm.

Pairwise K2P genetic distances for all analyzed *Cox1* sequences of *Novophytoptus* ranged from 0.20 to 0.35 (Table S1). The average K2P value between specimens of *Novophytoptus* included in the analysis was 0.23 ± 0.0.02 and that between specimens identified as *N. rostratae* was 0.21 ± 0.02. The lowest K2P distances between *Cox1* sequences of the two new species and other *Cox1 Novophytoptus* sequences were equal to 0.22 and were found in pairs with sequence KY922365 of *N. rostratae*.

## 4. Molecular Phylogenetic Analyses

Maximum likelihood analyses of *Cox1* sequences treated as nucleotides, codons, or amino acids produced similar topologies with most nodes having low support, indicating poor resolution of the obtained phylogenetic tree of *Novophytoptus*. Support values overall were slightly lower when treating *Cox1* as nucleotides or codons (not shown). In accordance with our previous study on the phylogeny of Phytoptidae [42], the genus *Novophytoptus* was inferred monophyletic (Figure 9). In all analyses, we observed the same pattern with sequences of the African *Novophytoptus* species forming a poorly supported clade and those of the Eurasian species forming a basal grade. *Novophytoptus* spp. associated with host–plant families Cyperaceae and Juncaceae were mixed in all trees and did not form host-family-specific clades.

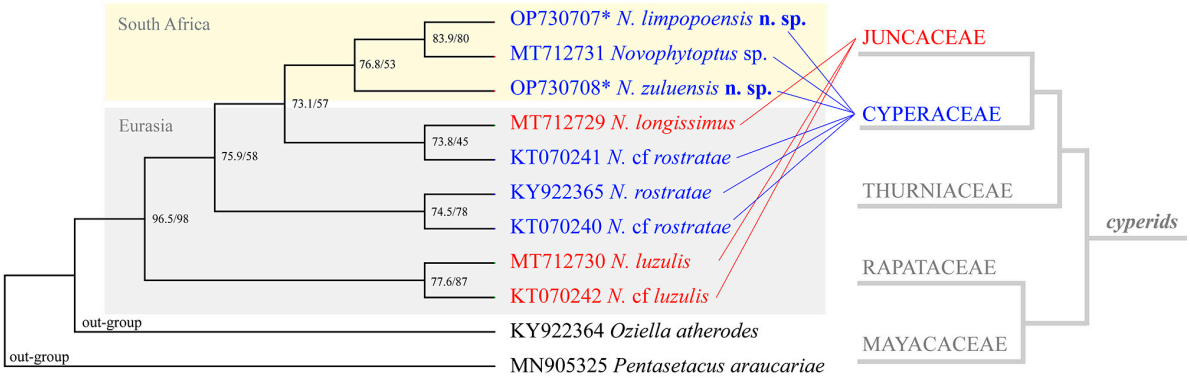


**Figure 9.** Maximum likelihood tree based on a 388-amino-acid alignment of the translated *Cox1* gene showing phylogeny of *Novophytoptus*. Nodes are labeled by values of SH-aLRT single branch test/UF bootstrap support (UFBS). Mite species associated with Cyperaceae and Juncaceae are colored blue and red, respectively. Two geographical groups of *Novophytoptus* species recorded from Africa and Eurasia are highlighted yellow and gray. Phylogeny of *cyperids* (simplified from [19]) is shown on the right. New sequences of *Novophytoptus* obtained in this study are indicated by asterisks.

## 5. Discussion

In this study, we described two new species of the endoparasitic genus *Novophytoptus* from South Africa, *N. limpopoensis* **n. sp.** and *N. zuluensis* **n. sp.**, and investigated the phylogeny of *Novophytoptus* through sequence analyses of the mitochondrial *Cox1* gene. Differentiating these new species required investigating the comparative material of three *Novophytoptus* spp. (*N. ammophillae*, *N. rostratae*, and *N. silvai*), which allowed us (1) to find characteristics for separating these *Novophytoptus* species and (2) observe that the ~20-years-old-type material of *N. silvai* from Brazil and of *N. ammophillae* from Poland are in very poor condition.

Similar to most eriophyoid genera, identification keys for species of *Novophytoptus* are lacking in the literature [43]. Although the total number of *Novophytoptus* species is relatively low (13), correct species identification is impeded by the great morphological similarity of *Novophytoptus* species and requires defining a set of reliable characteristics for species delimitation. Our study suggests the following morphological traits to be the most effective for this purpose and can be used in the future for preparing a key for *Novophytoptus* species: (a) ornamentation of coxae and prodorsal shield, especially presence of clusters of microtubercles and lengths of median, oblique, and L-shaped lines; (b) empodial morphology; (c) thickness of opisthosomal setae, especially setae *c2*, *d*, *e*, and *h1*; (d) presence/absence of microtubercles on dorsal telosomal annuli; (e) striation on ventral surface of leg segments, especially on tibiae; (f) some morphometrics, including lengths of body and setae *sc*, number of dorsal opisthosomal annuli, and the relative dimensions (width/length) of the body.

Barcode gene sequence comparison is a powerful contemporary method for testing conspecificity and species delimitation, and *Cox1* and *28S* genes are the most often and successfully used genes for Eriophyoidea [44–47]. In this study, we compared all available *Cox1* sequences of *Novophytoptus* and revealed that the high overall intergeneric sequence diversity averaged about 23%. We also found a pairwise sequence dissimilarity of 20–25% between members of morphologically distinct species (e.g., *N. longissimus* and *N. luzulis*) and between sequences of morphologically very similar mites from different populations of the same species (*N. rostratae*), suggesting cryptic speciation in *Novophytoptus*. A similarly high *Cox1* sequence diversity was observed in various eriophyoid genera and is common for complexes of cryptic species that evolved within different phylogenetically remote and ecologically diverse host plant groups [48–51].

Endoparasites have more intimate relationships with their hosts and are expected to show patterns of codivergence with hosts, more than ectoparasites [8]. In this study, we investigated the system "*Novophytoptus*—monocots" and expected to recover the codivergence of *Novophytoptus* with different families of Poales. Our molecular phylogenetic analyses included sequences of mite species from only two of the three monocot families reported to be hosts of *Novophytoptus*, namely Cyperaceae and Juncaceae (both from *cyperids*), while sequences of those from Poaceae (*graminids*) were unavailable. This limitation did not allow for testing the hypothesis on the codivergence of novophytoptines with higher lineages of Poales (*bromeliads*, *cyperids*, *graminids*, *restiids*, and *xyrids*) [19], yet the Cyperaceae/Juncaceae codivergence within *cyperids* was available for evaluation. Morphologically, *Novophytoptus* species from these two plant families are very similar; however, in general, *Novophytoptus* species from Juncaceae have prodorsal shields with more developed ornamentation, including more ridges and microtubercles.

Contrary to expectations, molecular phylogenetics has not shown family-host-specific clades of *Novophytoptus* but revealed geographic groups of *Novophytoptus* species collected from different continents (Africa and Eurasia) (Figure 9). A similar geographical lineage separation and absence of codiversification with hosts were obtained in a system comprising endoparasitic mermithid nematodes and stick insects *Timema* (Phasmatodea, Timematidae) and in some other, mostly aquatic, systems including flatworms and copepods associated with fish hosts [52]. The factors possibly contributing to the noncongruence of host and parasite trees include various traits of the parasite ecologies, higher mutation rates, smaller

effective population sizes, and limited dispersal abilities of endoparasites relative to their hosts [52]. Some of these factors, e.g., those related to dispersal and genetic drift, may be highly relevant to eriophyoids, especially to gall-forming and endoparasitic taxa such as *Novophytoptus* [53]. The latter is a rare example of an undoubtedly monophyletic eriophyoid taxon distinctly contrasting to most other eriophyoid genera morphologically and ecologically. We predict that dozens of new *Novophytoptus* species will be described in the future when more monocot hosts are examined for the presence of eriophyoids under the epidermis. The tentative results of the *Cox1* sequence phylogenetic analyses presented herein provide a basis for further coevolutionary studies on novophytoptines, which will be possible after more species and sequences of *Novophytoptus* from geographically remote regions and from phylogenetically distant hosts, representing all major clades of Poales, become available for analyses.

**Supplementary Materials:** The following supporting information can be downloaded at: https://www.mdpi.com/article/10.3390/d15030416/s1, Table S1: Pairwise K2P genetic distances between Cox1 sequences involved in the analyses.

**Author Contributions:** Conceptualization, P.E.C.; methodology, P.E.C.; validation, C.C., M.V.K., A.S.Z. and I.V.K.; formal analysis, P.E.C.; investigation, P.E.C., C.C., V.D.G. and I.V.K.; resources, data curation, M.V.K. and A.S.Z.; writing—original draft preparation, P.E.C.; writing—review and editing, P.E.C., V.D.G., C.C. and M.V.K.; visualization, P.E.C., V.D.G., M.V.K. and A.S.Z.; supervision, project administration, funding acquisition, P.E.C. and C.C. All authors have read and agreed to the published version of the manuscript.

**Funding:** This research was funded by the Ministry of Science and Higher Education of the Russian Federation (agreement 075-15-2022-322 "Agricultural technologies for the Future").

**Institutional Review Board Statement:** Not applicable.

**Data Availability Statement:** The new sequences of *Novophytoptus* have been deposited in the National Center for Biotechnology Information (NCBI) GenBank database (https://www.ncbi.nlm.nih.gov/genbank (accessed on 22 November 2022)); accession numbers: *OP730707* and *OP730708*.

**Acknowledgments:** We thank Evert E. Lindquist (Ottawa, Canada) for his remarks on the earlier version of the manuscript. We are grateful to C.H.W. Flechtmann and G.J. de Moraes (Escola Superior de Agricultura "Luiz de Queiroz" da Universidade de São Paulo (ESALQ/USP), Brazil) and A. Skoracka (A. Mickiewicz University, Poznan, Poland) for loaning paratypes. LM, PCR, and sequencing were performed using equipment of The Centre for Molecular and Cell Technologies and The Centre for Microscopy and Microanalysis of The Research Park of Saint-Petersburg State University (Russia).

**Conflicts of Interest:** The authors declare no conflict of interest. The funders had no role in the design of the study; in the collection, analyses, or interpretation of data; in the writing of the manuscript; or in the decision to publish the results.

## References

1. Oldfield, G.N. Diversity and host plant specificity. In *Eriophyoid Mites: Their Biology, Natural Enemies and Control. World Crop Pests 6*; Lindquist, E.E., Sabelis, M.W., Bruin, J., Eds.; Elsevier Science Publishing: Amsterdam, The Netherlands, 1996; Volume 6, pp. 199–216. [CrossRef]
2. Amrine, J.W., Jr.; Stasny, T.A.H.; Flechtmann, C.H.W. *Revised Keys to the World Genera of the Eriophyoidea (Acari: Prostigmata)*; Indira Publishing House: West Bloomfield, MI, USA, 2003; 244p.
3. Sullivan, G.; Ozman-Sullivan, S.K. Alarming evidence of widespread mite extinctions in the shadows of plant, insect and vertebrate extinctions. *Austral Ecol.* **2021**, *46*, 163–176. [CrossRef]
4. Lindquist, E.E. External anatomy and notation of structures. In *Eriophyoid Mites: Their Biology, Natural Enemies and Control. World Crop Pests 6*; Lindquist, E.E., Sabelis, M.W., Bruin, J., Eds.; Elsevier Science Publishing: Amsterdam, The Netherlands, 1996; Volume 6, pp. 3–31. [CrossRef]
5. Skoracka, A.; Smith, L.; Oldfield, G.; Cristofaro, M.; Amrine, J.W. Host-plant specificity and specialization in eriophyoid mites and their importance for the use of eriophyoid mites as biocontrol agents of weeds. *Exp. Appl. Acarol.* **2010**, *51*, 93–113. [CrossRef]

6. Paponova, S.S.; Chetverikov, P.E.; Pautov, A.A.; Yakovleva, O.V.; Zukoff, S.N.; Vishnyakov, A.E.; Sukhareva, S.I.; Krylova, E.G.; Dodueva, I.E.; Lutova, L.A. Gall mite *Fragariocoptes setiger* (Eriophyoidea) changes leaf developmental program and regulates gene expression in the leaf tissues of *Fragaria viridis* (Rosaceae). *Ann. Appl. Biol.* **2018**, *172*, 33–46. [CrossRef]
7. de Lillo, E.; Pozzebon, A.; Valenzano, D.; Duso, C. An intimate relationship between eriophyoid mites and their host plants–A review. *Front. Plant Sci.* **2018**, *9*, 1786. [CrossRef] [PubMed]
8. Poulin, R. *Evolutionary Ecology of Parasites*, 2nd ed.; Princeton University Press: Princeton, NJ, USA, 2011; 360p. [CrossRef]
9. Dowling, A. The evolution of parasitism and host associations in mites. In *Parasite Diversity and Diversification: Evolutionary Ecology Meets Phylogenetics*; Morand, S., Krasnov, B., Littlewood, D., Eds.; Cambridge University Press: Cambridge, UK, 2015; pp. 265–288. [CrossRef]
10. Krantz, G.W. Habit and Habitats. In *A manual of Acarology*, 3rd ed.; Krantz, G.W., Walter, D.E., Eds.; Texas Tech University Press: Lubbock, TX, USA, 2009; pp. 64–82.
11. Nuzzaci, G.; Alberti, G. Internal anatomy and physiology. In *Eriophyoid Mites: Their Biology, Natural Enemies and Control. World Crop Pests 6*; Lindquist, E.E., Sabelis, M.W., Bruin, J., Eds.; Elsevier Science Publishing: Amsterdam, The Netherlands, 1996; Volume 6, pp. 101–150. [CrossRef]
12. Sidorchuk, E.A.; Schmidt, A.R.; Ragazzi, E.; Roghi, G.; Lindquist, E.E. Plant-feeding mite diversity in Triassic amber (Acari: Tetrapodili). *J. Syst. Palaeontol.* **2014**, *13*, 129–151. [CrossRef]
13. Bolton, S.J.; Bauchan, G.R.; Chetverikov, P.E.; Ochoa, R.; Klompen, H. A rudimentary sheath for the smallest of "biting" chelicerae: The mouthparts of Cunliffea (Nematalycidae) and a new hypothesis on the origin of the stylet sheath of Eriophyoidea (Acariformes). *Int. J. Acarol.* **2018**, *44*, 374–381. [CrossRef]
14. Bolton, S.J.; Chetverikov, P.E.; Klompen, H. Morphological support for a clade comprising two vermiform mite lineages: Eriophyoidea (Acariformes) and Nematalycidae (Acariformes). *Syst. Appl. Acarol.* **2017**, *22*, 1096–1131. [CrossRef]
15. Klimov, P.B.; Chetverikov, P.E.; Dodueva, I.E.; Vishnyakov, A.E.; Bolton, S.J.; Paponova, S.S.; Lutova, L.A.; Tolstikov, A.V. Symbiotic bacteria of the gall-inducing mite *Fragariocoptes setiger* (Eriophyoidea) and phylogenomic resolution of the eriophyoid position among Acari. *Sci. Rep. UK* **2022**, *12*, 3811. [CrossRef]
16. Haupt, J.; Coineau, Y. Ultrastructure and functional morphology of a nematalycid mite (Acari: Actinotrichida: Endostigmata: Nematalycidae): Adaptations to mesopsammal life. *Acta Zool.* **1999**, *80*, 97–112. [CrossRef]
17. Chetverikov, P.E. Hidden diversity of endoparasitic eriophyoid mites: Two new *Novophytoptus* Roivainen, 1947 (Acari: Eriophyoidea: Phytoptidae) species from the parenchymatous tissues of rushes (Juncaceae). *Zootaxa* **2015**, *4006*, 481–505. [CrossRef]
18. Chetverikov, P.E.; Amrine, J.; Bauchan, G.; Ochoa, R.; Sukhareva, S.I.; Vishnyakov, A.E. Supplementary description of *Novophytoptus stipae* Keifer 1962 (Acariformes, Eriophyoidea) with LT-SEM observation on mites from putatively conspecific populations: Cryptic speciation or polyphagy of novophytoptines on phylogenetically remote hosts? *Syst. Appl. Acarol.* **2017**, *22*, 253–270. [CrossRef]
19. Bouchenak-Khelladi, Y.; Muasya, A.M.; Linder, H.P. A revised evolutionary history of Poales: Origins and diversification. *Bot. J. Linn. Soc.* **2014**, *175*, 4–16. [CrossRef]
20. Flechtmann, C.H. Eriophyid mites (Acari: Eriophyidae) from Brazilian sedges (Cyperaceae). *Int. J. Acarol.* **2004**, *30*, 157–164. [CrossRef]
21. Amrine, J.W., Jr.; Manson, D.C.M. Preparation, mounting and descriptive study of eriophyoid mites. In *Eriophyoid Mites: Their Biology, Natural Enemies and Control. World Crop Pests 6*; Lindquist, E.E., Sabelis, M.W., Bruin, J., Eds.; Elsevier Science Publishing: Amsterdam, The Netherlands, 1996; Volume 6, pp. 383–396. [CrossRef]
22. Chetverikov, P.E. Video projector: A digital replacement for camera lucida for drawing mites and other microscopic objects. *Syst. Appl. Acarol.* **2016**, *21*, 1278–1280. [CrossRef]
23. Gehrke, B. Synopsis of *Carex* (Cyperaceae) from sub-Saharan Africa and Madagascar. *Bot. J. Linn. Soc.* **2011**, *166*, 51–99. [CrossRef]
24. Klimov, P.B.; OConnor, B.M.; Chetverikov, P.E.; Bolton, S.J.; Pepato, A.R.; Mortazavi, A.L.; Tolstikov, A.V.; Bauchan, G.R.; Ochoa, R. Comprehensive phylogeny of acariform mites (Acariformes) provides insights on the origin of the four-legged mites (Eriophyoidea), a long branch. *Mol. Phylogenet. Evol.* **2018**, *119*, 105–117. [CrossRef]
25. Katoh, K.; Misawa, K.; Kuma, K.; Miyata, T. MAFFT: A novel method for rapid multiple sequence alignment based on fast Fourier transformation. *Nucleic Acids Res.* **2002**, *30*, 3059–3066. [CrossRef] [PubMed]
26. Katoh, K.; Rozewicki, J.; Yamada, K.D. MAFFT online service: Multiple sequence alignment, interactive sequence choice and visualization. *Brief. Bioinform.* **2017**, *20*, 1160–1166. [CrossRef]
27. Kumar, S.; Stecher, G.; Tamura, K. MEGA7: Molecular evolutionary genetics analysis version 7.0 for bigger datasets. *Mol. Biol. Evol.* **2017**, *33*, 1870–1874. [CrossRef]
28. Minh, B.Q.; Schmidt, H.A.; Chernomor, O.; Schrempf, D.; Woodhams, M.D.; von Haeseler, A.; Lanfear, R. IQ-TREE 2: New Models and Efficient Methods for Phylogenetic Inference in the Genomic Era. *Mol. Biol. Evol.* **2020**, *37*, 1530–1534. [CrossRef] [PubMed]
29. Kalyaanamoorthy, S.; Minh, B.Q.; Wong, T.K.F.; von Haeseler, A.; Jermiin, L.S. ModelFinder: Fast model selection for accurate phylogenetic estimates. *Nat. Methods* **2017**, *14*, 587–589. [CrossRef] [PubMed]
30. Skoracka, A.; Boczek, J. *Novophytoptus glyceriae* sp. n. and *N. ammophilae* sp. n., the new species of eriophyoid mites (Acari: Eriophyoidea) from grasses. *Acarina* **2000**, *8*, 95–101.
31. Roivainen, H. Eriophyid news from Finland. *Entomol. Fenn.* **1947**, *3*, 1–51.

32. Chetverikov, P.E.; Sukhareva, S.I. Supplementary descriptions and biological notes on eriophyid mites (Acari: Eriophyidae) of the genus *Novophytoptus* Roivainen, 1947. *Acarina* **2007**, *15*, 261–268.
33. Petanović, R.; Chetverikov, P.; Smiljanić, D. Eriophyoid mites (Acari: Eriophyoidea) from sedges (*Carex* spp., Cyperaceae) in Serbia. *Acta Entomol. Serbica* **2007**, *12*, 107–113.
34. Skoracka, A.; Dabert, M. The cereal rust mite *Abacarus hystrix* (Acari: Eriophyoidea) is a complex of species: Evidence from mitochondrial and nuclear DNA sequences. *Bull. Entomol. Res.* **2010**, *100*, 263–272. [CrossRef] [PubMed]
35. Skoracka, A.; Kuczyński, L.; de Mendonça, R.S.; Dabert, M.; Szydło, W.; Knihinicki, D.; Truol, G.; Navia, D. Cryptic species within the wheat curl mite *Aceria tosichella* (Keifer)(Acari: Eriophyoidea), revealed by mitochondrial, nuclear and morphometric data. *Invertebr. Syst.* **2012**, *26*, 417–433. [CrossRef]
36. Smith, I.M. A new species of eriophyoid mite with eye-like structures, and remarks on the genus *Phytoptus* (Acari: Prostigmata: Phytoptidae). *Can. Entomol.* **1977**, *109*, 1097–1102. [CrossRef]
37. Flechtmann, C.H.; Arana, M.; Ciarrocchi, F.; Chetverikov, P.E.; Amrine, J.W., Jr. Rediscovery and redescription of two eriophyid mites (Acari, Prostigmata, Eriophyidae) from *Baccharis salicifolia* (Asteraceae), from Argentina with remarks on the eriophyoid coverflap base. *Acarologia* **2015**, *55*, 387–396. [CrossRef]
38. Lebrun, J.-P.; Stork, A.L. *Tropical African Flowering Plants: Ecology and Distribution*; Cyperaceae; Éditions des Conservatoire et Jardin Botaniques: Genève, Switzerland, 2020; Volume 11, 368p.
39. Herman, P.P.J.; Retief, E. Plants of thenorthern provinces of South Africa: Keys and diagnostic characters. *Strelitzia* **1997**, *6*, 1–681.
40. Retief, E.; Meyer, N.L. Cyperaceae. In *Plants of the Free State: Inventory and Identification Guide*; Retief, E., Meyer, N.L., Eds.; Strelitzia, South African National Biodiversity Institute: Pretoria, South Africa, 2017; Volume 38, pp. 875–904.
41. Global Plants. Available online: http://plants.jstor.org (accessed on 22 November 2022).
42. Chetverikov, P.E.; Craemer, C.; Cvrković, T.; Klimov, P.B.; Petanović, R.U.; Romanovich, A.E.; Sukhareva, S.I.; Zukoff, S.N.; Bolton, S.; Amrine, J. Molecular phylogeny of the phytoparasitic mite family Phytoptidae (Acariformes: Eriophyoidea) identified the female genitalic anatomy as a major macroevolutionary factor and revealed multiple origins of gall induction. *Exp. Appl. Acarol.* **2021**, *83*, 31–68. [CrossRef]
43. Lindquist, E.E.; Amrine, J.W., Jr. Systematics, diagnoses for major taxa, and keys to families and genera with species on plants of economic importance. In *Eriophyoid Mites: Their Biology, Natural Enemies and Control. World Crop Pests 6*; Lindquist, E.E., Sabelis, M.W., Bruin, J., Eds.; Elsevier Science Publishing: Amsterdam, The Netherlands, 1996; Volume 6, pp. 33–87. [CrossRef]
44. Guo, J.F.; Li, H.S.; Wang, B.; Xue, X.F.; Hong, X.Y. DNA barcoding reveals the protogyne and deutogyne of *Tegolophus celtis* sp. nov. (Acari: Eriophyidae). *Exp. Appl. Acarol.* **2015**, *67*, 393–410. [CrossRef]
45. Petanović, R. Towards an integrative approach to taxonomy of Eriophyoidea (Acari, Prostigmata)-An overview. *Ecol. Montenegrina* **2016**, *7*, 580–599. [CrossRef]
46. Druciarek, T.; Lewandowski, M.; Tzanetakis, I. A new, sensitive and efficient method for taxonomic placement in the Eriophyoidea and virus detection in individual eriophyoids. *Exp. Appl. Acarol.* **2019**, *78*, 247–261. [CrossRef]
47. Chetverikov, P.E.; Klimov, P.B.; He, Q. Vertical transmission and seasonal dimorphism of eriophyoid mites (Acariformes, Eriophyoidea) parasitic on the Norway maple: A case study. *Royal Soc. Open Sci.* **2022**, *9*, 220820. [CrossRef]
48. Skoracka, A.; Magalhaes, S.; Rector, B.G.; Kuczyński, L. Cryptic speciation in the Acari: A function of species lifestyles or our ability to separate species? *Exp. Appl. Acarol.* **2015**, *67*, 165–182. [CrossRef] [PubMed]
49. Druciarek, T.; Lewandowski, M.; Tzanetakis, I. Molecular phylogeny of *Phyllocoptes* associated with roses discloses the presence of a new species. *Infect. Genet. Evol.* **2021**, *95*, 105051. [CrossRef] [PubMed]
50. Cvrković, T.; Chetverikov, P.; Vidović, B.; Petanović, R. Cryptic speciation within *Phytoptus avellanae* s.l. (Eriophyoidea: Phytoptidae) revealed by molecular data and observations on molting *Tegonotus*-like nymphs. *Exp. Appl. Acarol.* **2016**, *68*, 83–96. [CrossRef]
51. Saccaggi, D.L.; Maboeei, P.; Powell, C.; Ngubane-Ndhlovu, N.P.; Allsopp, E.; Wesley-Smith, J.; van Asch, B. Towards Solving the "Colomerus vitis Conundrum": Genetic Evidence Reveals a Complex of Highly Diverged Groups with Little Morphological Differentiation. *Diversity* **2022**, *14*, 342. [CrossRef]
52. Larose, C.; Schwander, T. Nematode endoparasites do not codiversify with their stick insect hosts. *Ecol. Evol.* **2016**, *6*, 5446–5458. [CrossRef] [PubMed]
53. Sabelis, M.W.; Bruin, J. Evolutionary ecology: Life history patterns, food plant choice and dispersal. In *Eriophyoid Mites: Their Biology, Natural Enemies and Control. World Crop Pests 6*; Lindquist, E.E., Sabelis, M.W., Bruin, J., Eds.; Elsevier Science Publishing: Amsterdam, The Netherlands, 1996; Volume 6, pp. 329–366.